AMERICAN SOCIETY FOR MICROBIOLOGY | Antimicrobial Agents and Chemotherapy®

EXPERIMENTAL THERAPEUTICS

In Vitro and *In Vivo* Drug-Drug Interaction Study of the Effects of Ivermectin and Oxantel Pamoate on Tribendimidine

Anna Neodo,[a,b] Jessica D. Schulz,[a,b] Jörg Huwyler,[c] Jennifer Keiser[a,b]

[a]Department of Medical Parasitology and Infection Biology, Swiss Tropical and Public Health Institute, Basel, Switzerland
[b]University of Basel, Basel, Switzerland
[c]Department of Pharmaceutical Sciences, Division of Pharmaceutical Technology, University of Basel, Basel, Switzerland

ABSTRACT Soil-transmitted helminth (STH) infections still remain a major health problem in poor rural settings. The lack of efficacious drugs against all STH species raises interest in drug combinations. Drug-drug interactions (DDIs) are, however, of major concern, so careful *in vitro* and *in vivo* characterization is needed. The combination of tribendimidine with either ivermectin or oxantel pamoate targets a broad range of STHs and thus represents a promising treatment alternative. Drug-drug interactions, however, have not yet been investigated. Therefore, the effects of combinations of ivermectin, oxantel pamoate, and tribendimidine's active metabolite deacylated amidantel (dADT) on cytochrome P450 (CYP450) metabolism were evaluated, followed by a pharmacokinetic analysis of tribendimidine and ivermectin alone and in combination in healthy rats. Oxantel pamoate is only poorly absorbed and was therefore excluded from pharmacokinetic analysis. No evident effect was observed for tribendimidine-oxantel pamoate at the CYP450 metabolism level, whereas a combination of tribendimidine and ivermectin led to moderately increased CYP2D6 inhibition compared to ivermectin or tribendimidine alone. Coadministration of tribendimidine with ivermectin altered neither the time to maximum concentration of drug in plasma (T_{max}) nor the elimination half-lives of dADT, the acetylated derivative of amidantel (adADT), and ivermectin. While the area under the concentration-versus-time curve (AUC) and maximum concentration of drug in plasma (C_{max}) values of dADT, adADT, and ivermectin are reduced by coadministration, the change is insufficient to declare that a DDI has been detected. Further studies are necessary to understand the observed interaction of tribendimidine and ivermectin, which is not related to P450 metabolism, and its significance for the situation in humans.

KEYWORDS CYP450, drug interaction, tribendimidine

Soil-transmitted helminths (STHs) afflict almost a billion people, mostly in low-income tropical and subtropical areas (1, 2). The majority of individuals are parasitized with one or more of the following STH species: the roundworm *Ascaris lumbricoides*, the whipworm *Trichuris trichiura*, the hookworms *Ancylostoma duodenale* and *Necator americanus*, and the threadworm *Strongyloides stercoralis* (2). STHs are particularly detrimental to children, pregnant women, and infants, as these infections lead to malnutrition and anemia and impair cognitive and physical development (3, 4). In total, the global impact of STH infections has been estimated at 3.3 million disability-adjusted life years (DALYs) (5).

Currently, five major drugs, albendazole, mebendazole, levamisole, pyrantel pamoate, and ivermectin, are used for helminth infections in humans (6, 7). Mass drug administration programs, so-called preventive chemotherapy, rely mostly on albendazole and mebendazole to control STH morbidity and transmission. With a single oral

Citation Neodo A, Schulz JD, Huwyler J, Keiser J. 2019. *In vitro* and *in vivo* drug-drug interaction study of the effects of ivermectin and oxantel pamoate on tribendimidine. Antimicrob Agents Chemother 63:e00762-18. https://doi.org/10.1128/AAC.00762-18.

Address correspondence to Jennifer Keiser, jennifer.keiser@swisstph.ch.

Received 16 April 2018
Returned for modification 5 July 2018
Accepted 10 October 2018
Accepted manuscript posted online 15 October 2018
Published 21 December 2018

dose, both drugs are effective against *A. lumbricoides* and hookworms yet have low efficacy against *T. trichiura* infections (6). Levamisole and pyrantel pamoate possess similar anthelmintic activity spectra, but they are less frequently used due to the need for weight dosing (6). Moreover, ivermectin has particularly high efficacy against STH infections with *S. stercoralis* and *A. lumbricoides* (7, 8). In addition to above-mentioned drugs, tribendimidine and oxantel pamoate could be potentially valuable additions to deworming programs. Oxantel, an old veterinary drug developed in the 1970s with poor oral bioavailability (9), has little effect against *A. lumbricoides* and hookworms but has shown promising activity against *T. trichiura* (10). The newest human anthelmintic, tribendimidine, marketed in China since 2004, has proven to be a safe and a highly efficacious treatment for hookworm and *A. lumbricoides* infections (11).

Numerous drug combinations have been tested against STHs in recent years (12). Besides extending the activity spectrum, a successful combination would allow improvement of efficacy and deceleration of resistance. Indeed, albendazole plus ivermectin, albendazole plus oxantel pamoate, tribendimidine plus ivermectin, tribendimidine plus oxantel pamoate, as well as triple-drug therapy with albendazole plus oxantel pamoate plus pyrantel pamoate have revealed a broad spectrum of activity against STH infections in randomized controlled trials (12). Given that albendazole has been extensively used in deworming programs for years and the risk of resistance to it is increasing with every year (6), tribendimidine could potentially replace albendazole, as both compounds have similar activity spectra yet different mechanisms of action. Importantly, two previous studies in China and in Tanzania and Côte-d'Ivoire have both revealed increased efficacy for tribendimidine coadministered with ivermectin against STHs (13, 14). It therefore would be of great interest to investigate the behavior of tribendimidine coadministered with other anti-STH drugs, in particular ivermectin and oxantel pamoate, in more detail.

Drug-drug interactions (DDIs) are a critical factor to consider when evaluating the safety and efficacy of drug combinations. Pharmacokinetic (PK) DDIs can often be explained by the effect that each drug has on a particular enzyme, membrane drug transporter, and plasma transport protein. A large portion of such DDIs arises during metabolism, for which the cytochrome P450 (CYP450) enzyme superfamily is primarily responsible (15). Depending on the drug combination, non-CYP metabolic enzymes and drug transporters can also contribute to DDIs (16, 43). For example, in animals, ivermectin DDIs originate mainly at the level of the P-glycoprotein transporter (ABCB1) that facilitates ivermectin biliary and intestinal excretion and prevents it from entering the central nervous system (17, 18). ABCB1 inhibitors therefore increase ivermectin concentrations in blood and cause neurotoxicity (e.g., spinosad in dogs) (19). Other transporters might also be involved in ivermectin DDIs: *in vitro* interactions with multidrug resistance-associated proteins (MRPs) and breast cancer resistance protein (BCRP) have been described (20, 21).

Little is known about tribendimidine DDIs. Several *in vitro* and *in vivo* studies using nematode models have suggested possible effects of interactions between tribendimidine and other antiparasitic compounds, including albendazole, levamisole, ivermectin, cyclooctadepsipeptide PF1022A, emodepside, and crystal proteins (22–25). Whether drug effects were additive, synergistic, or antagonistic varied widely depending on the compound and the parasite and in some cases reversed between *in vitro* and *in vivo* models. However, PK and CYP studies have not been conducted to date. Thus, tribendimidine DDIs remain yet to be identified, and the underlying mechanisms remain to be understood.

In this study, we explored potential DDIs of tribendimidine with either ivermectin or oxantel pamoate. The effect of each drug on each other's CYP450 metabolism was evaluated for major isoforms (CYP1A2, CYP2C9, CYP2D6, CYP2C19, and CYP3A4) via *in vitro* enzyme assays. Tribendimidine and ivermectin PK were monitored in healthy rats following separate administration or coadministration. Since, as mentioned above, oxantel pamoate is only poorly absorbed (9), possible DDIs would occur in the

TABLE 1 CYP450 inhibition (IC_{50} values) by dADT, ivermectin, oxantel, dADT plus ivermectin, and dADT plus oxantel pamoate *in vitro*

Enzyme	Median IC_{50} (μM) (range)					
	dADT	Ivermectin	dADT + ivermectin	Oxantel pamoate	dADT + oxantel pamoate	Positive control
CYP1A2	>100	>10	>100	9.0 (7.4–11.1)	9.3 (7.9–10.8)	0.5 (0.4–0.7) (propranolol)
CYP2C9	>100	5.3 (4.5–6.2)	6.9 (5.6–8.5)	1.4 (1.2–1.7)	0.8 (0.5–1.1)	2.1 (1.9–2.4) (diclofenac)
CYP2D6	>100	13.8 (10.0–27.1)	1.4 (0.8–2.6)	0.6 (0.5–0.6)	0.3 (0.2–0.4)	<0.03 (quinidine)
CYP2C19	>100	6.7 (5.3–8.9)	4.6 (3.2–7.0)	15.6 (13.6–17.8)	13.1 (11.5–14.9)	1.6 (1.4–1.8) (omeprazole)
CYP3A4	>100	11.3 (9.1–19.8)	10.2 (8.3–14.4)	13.9 (11.6–16.6)	13.8 (11.9–16.0)	0.006 (0.004–0.008) (ketoconazole)

gastrointestinal (GI) tract only; hence, PK interaction studies were not conducted for this drug.

RESULTS AND DISCUSSION

***In vitro* CYP inhibition.** In the literature, intact tribendimidine has been described in only one study (11), while only the metabolites were quantified in blood, urine, and fecal samples in rodents and humans in the remainder of the studies conducted to date (25–27). It has been suggested that tribendimidine rapidly breaks down by pH or that enzymes and/or bacteria of the GI tract cleave it into active deacylated amidantel (dADT) and inactive terephthalaldehyde (TPAL) (26, 27). We therefore used dADT rather than tribendimidine to evaluate CYP450-related DDIs of tribendimidine. In this study, dADT showed no effect on major CYP450 isoforms (CYP1A2, CYP2C9, CYP2D6, CYP2C19, and CYP3A4) at concentrations of up to 100 μM (Table 1; see also Fig. S1 to S10 in the supplemental material). It is therefore unlikely for dADT to interfere with CYP450-dependent metabolism of oxantel or ivermectin. Oxantel pamoate showed inhibitory activity against CYP2C9 and CYP2D6. The inhibition of CYP1A2, CYP2C19, and CYP3A4 by oxantel pamoate was more pronounced than in a previous study, which reported no interaction of oxantel pamoate with these enzymes (9). It should be noted, however, that it is very difficult to compare 50% inhibitory concentration (IC_{50}) values from different studies, since this parameter strongly depends on experimental conditions and, thus, the test system used (28). However, both studies confirm the low potential of oxantel pamoate to interact with CYP450 in view of the low plasma exposure of the compound *in vivo*.

Ivermectin undergoes relatively little metabolism, most of which is performed by CYP3A4 in the liver (29). We observed that ivermectin moderately inhibited CYP2C9, CYP2D6, CYP2C19, and CYP3A4 with IC_{50} values of 5.3 to 13.8 μM but not CYP1A2. Combining ivermectin with dADT produced no effect on any CYP450 except CYP2D6, where the IC_{50} decreased from 13.8 μM (range, 10.0 to 27.1 μM) for ivermectin alone to 1.4 μM (range, 0.8 to 2.6 μM) in combination. However, this interaction has no relevance for the *in vivo* situation since blood plasma concentrations of ivermectin reported in humans are rarely higher than 100 ng/ml (about 0.1 μM) at a standard oral dose (40).

We also verified the impact of dADT and oxantel coincubation; however, values calculated for oxantel pamoate plus dADT were similar to those for monotherapy. Hence, no CYP450-based DDIs were observed for dADT and oxantel pamoate, while dADT plus ivermectin synergistically inhibited CYP2D6. In view of the low ivermectin blood levels, however, we conclude that the risk for CYP450-mediated DDIs *in vivo* is minimal.

***In vivo* pharmacokinetics.** Our previous study of oxantel pamoate in rats has shown a very low bioavailability, below our limit of detection (9); thus, only the combination of tribendimidine plus ivermectin was evaluated *in vivo*. As mentioned above, only one PK study in rats reported a very low concentration of tribendimidine itself (maximum concentration of drug in plasma [C_{max}] of 381 ng/ml after a single oral dose of 150 mg/kg of body weight), a rapid peak (1.78 h), and rapid elimination (1.42 h) (30). However, details on the analytical method were not provided in that review article.

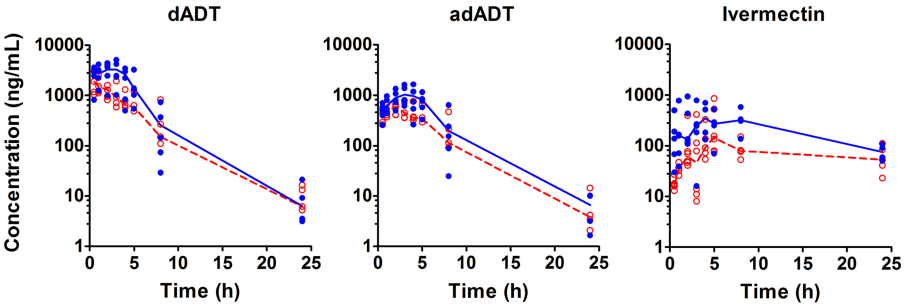

FIG 1 PK profiles of dADT, adADT, and ivermectin in rat plasma following a single oral dose of either tribendimidine (100 mg/kg), ivermectin (2.5 mg/kg), or both (at the same doses) administered to four, six, and six rats, respectively. Individual rats' concentrations are shown as circles, and median concentrations are traced as lines. Blue filled circles and solid lines, monotherapy; red empty circles and dashed lines, combination therapy.

On the other hand, Kulke et al. did not detect any tribendimidine in rat plasma (25). *In vivo* experiments with ^{14}C-labeled tribendimidine demonstrated that the active metabolite dADT was eliminated in a mostly unchanged form or as an acetylated derivative (adADT). Glucorinated dADT as well as hydroxylated adADT and demethylated adADT also have been observed as minor metabolites (31). In humans, tribendimidine is rapidly converted into dADT (11, 26, 32, 33), and in the case of *Opisthorchis viverrini*-infected adults, higher dADT exposure was associated with a high cure rate (33).

In our study, rats received a single oral dose of either tribendimidine (100 mg/kg), ivermectin (2.5 mg/kg), or both (tribendimidine at 100 mg/kg and ivermectin at 2.5 mg/kg). These doses in rats are roughly equivalent to 13.8 mg/kg of tribendimidine and 0.35 mg/kg of ivermectin in humans, respectively (34), in accordance with human dosages of 400 mg tribendimidine and 200 μg/kg ivermectin (6). Ivermectin, dADT, and adADT concentrations were then monitored for 24 h (Fig. 1). Analytical methods previously developed to quantify these compounds in human blood plasma were revalidated for rat plasma. Collected PK data were analyzed using a noncompartmental approach (Table 2).

Both dADT and adADT concentrations peaked at 2 h (time to maximum concentration of drug in serum [T_{max}]) and decreased by half (noncompartmental half-life [$t_{1/2}$]) in 2 to 3 h, similarly to previously reported dADT and adADT PK in rats (25).

As expected, T_{max} and $t_{1/2}$ of dADT and adADT in rats are shorter than those in adult humans (~8 to 10 h for T_{max} and ~4 to 6 h for $t_{1/2}$) (33). In terms of dADT exposure, the area under the concentration-versus-time curve (AUC) measured in rats corresponded well to the estimates extrapolated from PK data in adult humans. A 2-fold increase in the dADT AUC compared to that for humans (20,097 versus 11,668 ng h/ml [400 mg])

TABLE 2 Noncompartmental PK parameters for dADT, adADT, and ivermectin after oral administration of either tribendimidine (100 mg/kg, $n = 4$), ivermectin (2.5 mg/kg, $n = 6$), or both ($n = 6$) to healthy rats

	Median value for analyte (range)[a]					
	dADT		adADT		Ivermectin	
Parameter	Monotherapy	Combination	Monotherapy	Combination	Monotherapy	Combination
AUC_{0-t} (ng h/ml)	20,097 (13,216–20,331)	9,796 (4,362–13,218)	8,190 (6,654–9,482)	3,417 (3,055–6,805)	5,307 (2,195–11,236)	1,633 (1,099–7,616)
C_{max} (ng/ml)	4,040 (1,252–5060)	2,414 (1,160–4,000)	768 (652–1,641)	776 (468–2,476)	419 (137–932)	151 (79–854)
T_{max} (h)	2.0 (0.5–5.0)	2.0 (0.5–4.0)	2.0 (0.5–5.0)	2.0 (0.5–5.0)	6.5 (2.0–8.0)	5.0 (4.0–8.0)
$t_{1/2}$ (h)	2.6 (2.0–4.1)	3.0 (1.7–5.2)	3.3 (2.8–4.6)	3.4 (2.0–4.5)	11.2 (8.1–14.1)	11.4 (8.1–31.1)

[a]For dADT, the median AUC ratio (ratio of the AUC of the drug in combination to the AUC of the drug alone) was 0.925 (range, 0.890 to 0.960), and the median C_{max} ratio (ratio of the C_{max} of the drug in combination to the C_{max} of the drug alone) was 0.962 (range, 0.911 to 1.013); for adADT, the median AUC ratio was 0.925 (range, 0.894 to 0.956), and the median C_{max} ratio was 1.003 (range, 0.925 to 1.085); and for ivermectin, the median AUC ratio was 0.860 (range, 0.796 to 0.927), and the median C_{max} ratio was 0.885 (range, 0.745 to 1.032) (logarithmically transformed data).

(33) was expected (assuming a linear correlation of AUC with dose), given the slightly higher dose used in rats than in humans.

Ivermectin, generally known for its low plasma clearance and accumulation in fat tissues (35), needed 5 to 6.5 h to reach C_{max} and about 11 h to subside to half of it. Similar trends were observed previously in other species (35). Comparable T_{max} values were reported for ivermectin-treated dogs and rabbits (4.1 and 2.5 to 9.0 h, respectively), yet the half-life extended to about 3 days. PK parameters in ruminants show a larger deviation from our reported data (e.g., T_{max} of 16 to 44 h). In humans, the ivermectin concentration generally peaks around 3 to 6 h after oral administration and decreases with a half-life of 11 to 16 h, although a few studies have reported longer T_{max} and $t_{1/2}$ (10 h and 35 to 54 h, respectively) (36). Ivermectin human AUC values found in the literature sometimes vary 3- to 5-fold for the same or similar doses; however, some of them are in line with our *in vivo* data (37).

Coadministration of tribendimidine with ivermectin altered neither the T_{max} nor elimination half-lives of dADT, adADT, and ivermectin. While the AUCs and C_{max} of dADT, adADT, and ivermectin are reduced by coadministration, the change is insufficient to declare that a DDI has been detected (Fig. 1 and Table 2). Whether significant AUC and C_{max} changes actually occur in humans remains yet to be confirmed.

Tribendimidine-ivermectin and tribendimidine-oxantel pamoate are promising drug combinations for the treatment of STH infections, yet *in vitro* and *in vivo* DDI studies have not been conducted to date. No evident interaction was observed for tribendimidine plus oxantel pamoate with regard to CYP450 metabolism. Despite the observed moderate *in vitro* interactions between the two compounds at CYP2D6, tribendimidine and ivermectin do not significantly alter the pharmacokinetic behavior of each other in rats; hence, a clinically relevant interaction between tribendimidine and ivermectin seems to be unlikely. However, clinical trials will be needed to explore PK parameters of tribendimidine-ivermectin and tribendimidine-oxantel pamoate combinations and to confirm that these combinations are safe for large-scale clinical use in humans.

MATERIALS AND METHODS

Chemicals and reagents. Tribendimidine, dADT [*N*′-(4-aminophenyl)-*N*,*N*-dimethylacetamidine], and adADT [*N*′-(4-acetylaminophenyl)-*N*,*N*-dimethylacetamidine] were provided by Shandong Xinhua Pharmaceutical Company (Zibo, People's Republic of China). Deuterated internal standards (ISs), ivermectin-d_2, dADT-d_6, and adADT-d_6, were ordered from Toronto Research Chemicals (Ontario, Canada). Acetonitrile of liquid chromatography-mass spectrometry (LC-MS) grade (Rotisolv) was acquired from Carl Roth GmbH (Karlsruhe, Germany). Ultrapure water was obtained with a Millipore Milli-Q water purification system. Ivermectin, dimethyl sulfoxide (DMSO), ammonium acetate, and formic acid (LC-MS grade) were purchased from Sigma-Aldrich (Buchs, Switzerland). Vivid CYP450 screening kits were purchased from Life Technologies (Carlsbad, CA, USA). Blank rat plasma was obtained from Dunn Labortechnik GmbH (Asbach, Germany). Blank rat plasma for quality control (QC) samples was prepared by centrifugation from blood collected from six different rats (Charles River, Sulzfeld, Germany) into Li-heparin tubes by cardiac puncture. SOLAμ solid-phase extraction (SPE) plates were acquired from Thermo Fischer Scientific (Reinach, Germany). Protein low-binding material was used for ivermectin (Vadaux-Eppendorf AG, Basel, Switzerland).

CYP450 inhibition screening. Commercially available fluorogenic human recombinant Vivid CYP450 screening kits (CYP1A2 7-ethoxy-methyloxy-3-cyanocoumarin, CYP3A4 benzyloxy-methylresorufin, CYP2C19 7-ethoxy-methyloxy-3-cyanocoumarin, and CYP2D6 7-*p*-methoxy-benzyloxy-4-trifluorocoumarin) were used to assess tribendimidine DDIs with ivermectin and oxantel pamoate at the level of CYP450 metabolism *in vitro*. We followed the kit's user guide (9). Drug stock solutions (10 mM for dADT, 10 mM for oxantel pamoate, and 1 mM for ivermectin) were prepared in DMSO. Stock solutions were used to prepare working solutions of compounds in assay reaction buffer (0.34, 1.0, 3.1, 9.3, 27.8, 83.3, and 250 μM for dADT and oxantel pamoate and 0.034, 0.1, 0.3, 0.9, 2, 8, 8.3, and 25 μM for ivermectin). The enzyme (50 μl) was incubated with working solution (40 μl) for 10 min. The fluorogenic substrate and $NADP^+$ (10 μl) were then added, and fluorescence was monitored over time (kinetic assay mode). dADT and oxantel pamoate were thus tested at a concentration range of 0.14 to 100 μM, and ivermectin was evaluated at a concentration range of 0.014 to 10 μM. The final concentration of DMSO in the assay mixture was 1%. The assays were run in duplicate and performed twice. The reaction rate was quantified as the slope of the linear range of the fluorescence-versus-time curve. Percent inhibition was then calculated as $100\% \times [1 - (X - P)/(N - P)]$, where X is the rate for the test compound, P is the rate for the positive control, and N is the rate for the solvent control. With percent inhibition at various concentrations, IC_{50} values were calculated by Prism (7.0a; GraphPad).

***In vivo* pharmacokinetic studies.** All animal experiments were approved by local and national veterinary agencies (license 2070). Male rats [140 to 185 g, Crl:WI(Han) strain, 3 weeks old] with a jugular

vein catheter (PinPort access) were acquired from Charles River (Sulzfeld, Germany) and kept at 22°C, with 50% humidity, a 12-h light-and-dark cycle, and free access to rodent food and water. For oral administration, tribendimidine, ivermectin, and their combination were prepared as suspensions in a Tween 80-ethanol (EtOH)-water mix (7%, 3%, and 90%, vol/vol/vol). Rats, which had been fasted overnight, were treated with either 100 mg/kg of tribendimidine (four rats) (38), 2.5 mg/kg of ivermectin (six rats) (39), or a combination of both drugs (six rats) at the same doses. Blood samples were withdrawn at 0.5, 1, 2, 3, 4, 5, 8, and 24 h posttreatment.

Blood samples were collected into lithium heparin-coated tubes using a 1-ml syringe and centrifuged at 9,000 rpm (4,980 × *g*) for 10 min. Obtained plasma samples were stored at −20°C prior to analysis.

Sample preparation for tribendimidine analysis. Stock 10-mg/ml solutions of dADT, adADT, dADT-d_6 (IS), and adADT-d_6 (IS) were prepared in acetonitrile. Working solutions (50, 25, 5, 2.5, 1.25, 0.5, 0.25, and 0.125 μg/ml) were obtained by serial dilution in acetonitrile. Blank rat plasma (98 μl/sample) was then spiked with working solutions (2 μl/sample) to produce calibration standards (1,000, 500, 100, 50, 25, 10, 5, and 2.5 ng/ml) and quality control (QC) samples (750, 125, 4.5, and 2.5 ng/ml). Each quality control was prepared in six replicates. Calibration and QC samples, as well as plasma samples collected during the PK study, were diluted 1:4 with IS solution in acetonitrile (10 ng/ml). They were then vortexed (2 s), shaken for 10 min (25°C at a 1,400-rpm shaking speed), and centrifuged for 10 min (15,000 rpm or 15,093 × *g* at 10°C). The supernatant was pipetted into 96-multiwell plates (deep well, 500 μl; Eppendorf) closed with SepraSeal presplit caps (Thermo Scientific) and kept at 10°C in the autosampler. As the first analysis revealed that PK samples collected from 0.5 to 8 h often exceeded the upper limit of quantification (ULOQ), these samples were diluted 4-fold with blank rat plasma prior to sample preparation.

LC-MS/MS equipment, conditions, and method revalidation procedure for tribendimidine. The high-performance liquid chromatography (HPLC) system (Shimadzu, Kyoto, Japan) included two LC-20AD pumps, an online DG-3310 degasser (Sanwa Tsusho, Tokyo, Japan), a CTC HTS PAL autosampler (CTC Analytics, Zwingen, Switzerland), and a 10-port injection valve (VICI Valco Instruments, Schenkon, Switzerland) with a 2-μl loop. The analytical method was adapted from a previously reported procedure (26). Chromatographic separation was achieved at 20°C at a 0.3-ml/min flow rate using a Phenomenex pentafluorophenyl 5-μm, 50- by 2.0-mm column (Brechbüler AG, Schlieren, Switzerland) with 10 mM ammonium acetate and 0.15% HCOOH in water (solvent A) and with 10 mM ammonium acetate and 0.15% HCOOH in acetonitrile-water in a 9:1 mixture (solvent B). The following solvent gradient was used: t = 0 min, B = 90%; 2.5 min, B = 90%; 3 min, B = 5%; 4 min, B = 5%; 4.5 min, B = 90%; 6 min, B = 90%. The flow from the HPLC column was diverted to the MS instrument (10-port valve; VICI Valco Instruments, Schenkon, Switzerland) during the interval from 0.5 to 1.4 min when analytes were eluted. An API 3200 instrument (AB Sciex, Framingham, MA, USA) with a TurboIon spray source was used to detect the analytes in positive mode by multiple-reaction monitoring. Signals were optimized by tandem mass spectrometry (MS/MS) parameter optimization (see Table S1 in the supplemental material). The same MS/MS parameters were used for deuterated internal standards as for the corresponding analytes.

We revalidated this method for rat plasma and with slightly modified equipment (AP 3200 instead of AP 3000 and column width of 2 mm instead of 4.6 mm). Three calibration lines and sets of QCs were prepared on the same day to assess intraday accuracy and precision. On two other days, another calibration line and set of QCs were analyzed to evaluate interday accuracy and precision. On one of these three days, a set of QCs prepared in pure water and a set of QCs prepared by using a plasma extract were analyzed to measure extraction efficiency and possible matrix effects. Analyte peak areas were normalized to the peak area of the corresponding deuterated IS. Calibration curves were fitted by linear regression with $1/x^2$ weighting. The accuracy, precision, matrix effects, and extraction efficiency were accepted within a range of 85% to 115% (80% to 120% for the lower limit of quantification [LLOQ]) (data not shown).

LC-MS/MS equipment and conditions for ivermectin analysis. Ivermectin analysis was performed according to methods described previously by Schulz et al. (40). Briefly, ivermectin (892.5 → 307 *m/z*) was detected by using a 1260 Infinity LC system connected to a 6460 triple-quadrupole LC-MS instrument (Agilent Technologies, Santa Clara, CA, USA). Separation was achieved on a Luna C_8 column (30 by 2 mm, 3 μm, 100 Å; Phenomenex, Torrance, CA, USA) using 0.4 mM ammonium acetate with 0.1% formic acid (mobile phase A) and acetonitrile with 0.1% formic acid (mobile phase B) at a flow rate of 0.5 ml/min. Mobile phase B was set to 40% for 0.2 min, increased to 95% for 0.3 min, maintained at 95% for 2 min, rapidly reset to 40% in 0.05 min, and maintained at 40% for 1.45 min. The injection volume was 10 μl.

To adapt the method for rat plasma, samples were diluted with human blood plasma (1:1, vol/vol). Plasma samples were mixed 1:1 (vol/vol) with acetonitrile-water (4:1, vol/vol), shaken for 10 min (2,000 rpm at room temperature [RT]), and centrifuged for 10 min at 3,000 × *g*. The supernatant was then loaded onto SPE plates, which were washed with acetonitrile-water (1:3, vol/vol). Ivermectin was eluted with acetonitrile (50 μl).

Pharmacokinetics and statistical analysis. Analyst 1.6.2. software (AB Sciex) was used to integrate LC-MS/MS signals; fit the calibration lines; and calculate concentrations, accuracies, and precisions. The area under the plasma concentration-versus-time curve until the last measured time point (AUC_{0-t}) was calculated using the linear trapezoidal rule. The noncompartmental half-life ($t_{1/2}$) was estimated by linear regression on semi-log-transformed data. The maximal plasma concentration (C_{max}) and time to reach it (T_{max}) were taken directly from the observed data. PK data were analyzed using the PK R language package (41). Noncompartmental PK parameters were first determined for each rat, and the medians (ranges) were then calculated. The data were logarithmically transformed, and a confidence interval (CI) approach was used to evaluate the drug combination effect on AUC and C_{max}. No DDIs were detected

if the 90% CI of the AUC ratio (in the presence and absence of the other drug) was within 0.8 to 1.25 and that of the C_{max} ratio was within 0.70 to 1.43 (42).

SUPPLEMENTAL MATERIAL

Supplemental material for this article may be found at https://doi.org/10.1128/AAC.00762-18.

SUPPLEMENTAL FILE 1, PDF file, 0.7 MB.

ACKNOWLEDGMENTS

We are grateful to Valérian Pasche and Noemi Hiroshige for help with the experiments.

We are grateful to the Swiss National Science Foundation for financial support (grant no. 320030_14930/1).

REFERENCES

1. Pullan RL, Brooker SJ. 2012. The global limits and population at risk of soil-transmitted helminth infections in 2010. Parasit Vectors 5:81. https://doi.org/10.1186/1756-3305-5-81.
2. Jourdan PM, Lamberton PHL, Fenwick A, Addiss DG. 2018. Soil-transmitted helminth infections. Lancet 391:252–265. https://doi.org/10.1016/s0140-6736(17)31930-x.
3. Hall A, Hewitt G, Tuffrey V, de Silva N. 2008. A review and meta-analysis of the impact of intestinal worms on child growth and nutrition. Matern Child Nutr 4:118–236. https://doi.org/10.1111/j.1740-8709.2007.00127.x.
4. World Health Organization. 2017. WHO guidelines approved by the Guidelines Review Committee, guideline: preventive chemotherapy to control soil-transmitted helminth infections in at-risk population groups. World Health Organization, Geneva, Switzerland.
5. Global Burden of Disease Collaborators. 2017. Global, regional, and national disability-adjusted life-years (DALYs) for 333 diseases and injuries and healthy life expectancy (HALE) for 195 countries and territories, 1990–2016: a systematic analysis for the Global Burden of Disease Study 2016. Lancet 390:1260–1344. https://doi.org/10.1016/S0140-6736(17)32130-X.
6. Moser W, Schindler C, Keiser J. 2017. Efficacy of recommended drugs against soil transmitted helminths: systematic review and network meta-analysis. BMJ 358:j4307. https://doi.org/10.1136/bmj.j4307.
7. Wimmersberger D, Coulibaly JT, Schulz J, Puchkow M, Huwyler J, N'Gbesso Y, Hattendorf J, Keiser J. 2018. Efficacy and safety of ivermectin against *Trichuris trichiura* in preschool- and school-aged children: a randomized controlled dose-finding trial. Clin Infect Dis 67:1247–1255. https://doi.org/10.1093/cid/ciy246.
8. Marti H, Haji HJ, Savioli L, Chwaya HM, Mgeni AF, Ameir JS, Hatz C. 1996. A comparative trial of a single-dose ivermectin versus three days of albendazole for treatment of *Strongyloides stercoralis* and other soil-transmitted helminth infections in children. Am J Trop Med Hyg 55:477–481. https://doi.org/10.4269/ajtmh.1996.55.477.
9. Cowan N, Vargas M, Keiser J. 2016. *In vitro* and *in vivo* drug interaction study of two lead combinations, oxantel pamoate plus albendazole and albendazole plus mebendazole, for the treatment of human soil-transmitted helminthiasis. Antimicrob Agents Chemother 60:6127–6133. https://doi.org/10.1128/AAC.01217-16.
10. Speich B, Ame SM, Ali SM, Alles R, Huwyler J, Hattendorf J, Utzinger J, Albonico M, Keiser J. 2014. Oxantel pamoate-albendazole for *Trichuris trichiura* infection. N Engl J Med 370:610–620. https://doi.org/10.1056/NEJMoa1301956.
11. Xiao SH, Utzinger J, Tanner M, Keiser J, Xue J. 2013. Advances with the Chinese anthelminthic drug tribendimidine in clinical trials and laboratory investigations. Acta Trop 126:115–126. https://doi.org/10.1016/j.actatropica.2013.01.009.
12. Moser W, Schindler C, Keiser J. 7 September 2018. Drug combinations against soil-transmitted helminth infections. Adv Parasitol https://doi.org/10.1016/bs.apar.2018.08.002.
13. Wu Z-X, Qian Y. 2003. Therapeutic effect of tribendimidine combined with ivermectin against human intestinal nematode infection. J Pract Parasit Dis 2003:59–61.
14. Moser W, Coulibaly JT, Ali SM, Ame SM, Amour AK, Yapi RB, Albonico M, Puchkov M, Huwyler J, Hattendorf J, Keiser J. 2017. Efficacy and safety of tribendimidine, tribendimidine plus ivermectin, tribendimidine plus oxantel pamoate, and albendazole plus oxantel pamoate against hookworm and concomitant soil-transmitted helminth infections in Tanzania and Côte d'Ivoire: a randomised, controlled, single-blinded, non-inferiority trial. Lancet Infect Dis 17:1162–1171. https://doi.org/10.1016/S1473-3099(17)30487-5.
15. Fowler S, Morcos PN, Cleary Y, Martin-Facklam M, Parrott N, Gertz M, Yu L. 2017. Progress in prediction and interpretation of clinically relevant metabolic drug-drug interactions: a minireview illustrating recent developments and current opportunities. Curr Pharmacol Rep 3:36–49. https://doi.org/10.1007/s40495-017-0082-5.
16. Zhang L, Reynolds KS, Zhao P, Huang SM. 2010. Drug interactions evaluation: an integrated part of risk assessment of therapeutics. Toxicol Appl Pharmacol 243:134–145. https://doi.org/10.1016/j.taap.2009.12.016.
17. Ballent M, Lifschitz A, Virkel G, Sallovitz J, Lanusse C. 2006. Modulation of the P-glycoprotein-mediated intestinal secretion of ivermectin: *in vitro* and *in vivo* assessments. Drug Metab Dispos 34:457–463. https://doi.org/10.1124/dmd.105.007757.
18. Ballent M, Lifschitz A, Virkel G, Sallovitz J, Lanusse C. 2007. Involvement of P-glycoprotein on ivermectin kinetic behaviour in sheep: itraconazole-mediated changes on gastrointestinal disposition. J Vet Pharmacol Ther 30:242–248. https://doi.org/10.1111/j.1365-2885.2007.00848.x.
19. Dunn ST, Hedges L, Sampson KE, Lai Y, Mahabir S, Balogh L, Locuson CW. 2011. Pharmacokinetic interaction of the antiparasitic agents ivermectin and spinosad in dogs. Drug Metab Dispos 39:789–795. https://doi.org/10.1124/dmd.110.034827.
20. Real R, Egido E, Perez M, Gonzalez-Lobato L, Barrera B, Prieto JG, Alvarez AI, Merino G. 2011. Involvement of breast cancer resistance protein (BCRP/ABCG2) in the secretion of danofloxacin into milk: interaction with ivermectin. J Vet Pharmacol Ther 34:313–321. https://doi.org/10.1111/j.1365-2885.2010.01241.x.
21. Jani M, Makai I, Kis E, Szabo P, Nagy T, Krajcsi P, Lespine A. 2011. Ivermectin interacts with human ABCG2. J Pharm Sci 100:94–97. https://doi.org/10.1002/jps.22262.
22. Hu Y, Platzer EG, Bellier A, Aroian RV. 2010. Discovery of a highly synergistic anthelmintic combination that shows mutual hypersusceptibility. Proc Natl Acad Sci U S A 107:5955–5960. https://doi.org/10.1073/pnas.0912327107.
23. Tritten L, Nwosu U, Vargas M, Keiser J. 2012. *In vitro* and *in vivo* efficacy of tribendimidine and its metabolites alone and in combination against the hookworms *Heligmosomoides bakeri* and *Ancylostoma ceylanicum*. Acta Trop 122:101–107. https://doi.org/10.1016/j.actatropica.2011.12.008.
24. Kulke D, Krucken J, Harder A, von Samson-Himmelstjerna G. 2014. Efficacy of cyclooctadepsipeptides and aminophenylamidines against larval, immature and mature adult stages of a parasitologically characterized trichurosis model in mice. PLoS Negl Trop Dis 8:e2698. https://doi.org/10.1371/journal.pntd.0002698.
25. Kulke D, Krucken J, Harder A, Krebber R, Fraatz K, Mehlhorn H, Von Samson-Himmelstjerna G. 2013. *In vivo* efficacy of PF1022A and nicotinic acetylcholine receptor agonists alone and in combination against *Nippostrongylus brasiliensis*. Parasitology 140:1252–1265. https://doi.org/10.1017/S0031182013000632.
26. Duthaler U, Keiser J, Huwyler J. 2015. LC-MS/MS method for the determination of two metabolites of tribendimidine, deacylated amidantel

and its acetylated metabolite in plasma, blood and dried blood spots. J Pharm Biomed Anal 105:163–173. https://doi.org/10.1016/j.jpba.2014.12.006.
27. Yuan G, Xu J, Qu T, Wang B, Zhang R, Wei C, Guo R. 2010. Metabolism and disposition of tribendimidine and its metabolites in healthy Chinese volunteers. Drugs R D 10:83–90. https://doi.org/10.2165/11539320-000000000-00000.
28. Fowler S, Zhang H. 2008. *In vitro* evaluation of reversible and irreversible cytochrome P450 inhibition: current status on methodologies and their utility for predicting drug-drug interactions. AAPS J 10:410–424. https://doi.org/10.1208/s12248-008-9042-7.
29. Zeng Z, Andrew NW, Arison BH, Luffer-Atlas D, Wang RW. 1998. Identification of cytochrome P4503A4 as the major enzyme responsible for the metabolism of ivermectin by human liver microsomes. Xenobiotica 28:313–321. https://doi.org/10.1080/004982598239597.
30. Xiao SH, Wu HM, Tanner M, Utzinger J, Chong W. 2005. Tribendimidine: a promising, safe and broad-spectrum anthelmintic agent from China. Acta Trop 94:1–14. https://doi.org/10.1016/j.actatropica.2005.01.013.
31. Fontana E, Pignatti A, Ghiglieri A, Battaglia R, Cinato F, Wang C, de Hostos E. 2013. Carbon-14 labelled tribendimidine, a broad-spectrum anthelmintic drug. J Labelled Comp Radiopharm 56:471–474. https://doi.org/10.1002/jlcr.3070.
32. Guiyan Y, Benjie W, Chunmin W, Rui Z, Ruichen G. 2008. LC-MS determination of p-(1-dimethylamino ethylimino)aniline: a metabolite of tribendimidine in human plasma. Chromatographia 68:139–142. https://doi.org/10.1365/s10337-008-0657-8.
33. Duthaler U, Sayasone S, Vanobbergen F, Penny M, Odermatt P, Huwyler J, Keiser J. 2016. Single-ascending-dose pharmacokinetic study of tribendimidine in *Opisthorchis viverrini*-infected patients. Antimicrob Agents Chemother 60:5705–5715. https://doi.org/10.1128/AAC.00992-16.
34. Nair AB, Jacob S. 2016. A simple practice guide for dose conversion between animals and human. J Basic Clin Pharm 7:27–31. https://doi.org/10.4103/0976-0105.177703.
35. González Canga A, Sahagún Prieto AM, Diez Liébana MJ, Fernández Martínez N, Sierra Vega M, García Vieitez JJ. 2009. The pharmacokinetics and metabolism of ivermectin in domestic animal species. Vet J 179:25–37. https://doi.org/10.1016/j.tvjl.2007.07.011.
36. González Canga A, Sahagún Prieto AM, Diez Liébana MJ, Fernández Martínez N, Sierra Vega M, García Vieitez JJ. 2008. The pharmacokinetics and interactions of ivermectin in humans—a mini-review. AAPS J 10:42–46. https://doi.org/10.1208/s12248-007-9000-9.
37. Baraka OZ, Mahmoud BM, Marschke CK, Geary TG, Homeida MM, Williams JF. 1996. Ivermectin distribution in the plasma and tissues of patients infected with *Onchocerca volvulus*. Eur J Clin Pharmacol 50:407–410. https://doi.org/10.1007/s002280050131.
38. Xiao SH, Jian X, Tanner M, Yong-Nian Z, Keiser J, Utzinger J, Hui-Qiang Q. 2008. Artemether, artesunate, praziquantel and tribendimidine administered singly at different dosages against *Clonorchis sinensis*: a comparative *in vivo* study. Acta Trop 106:54–59. https://doi.org/10.1016/j.actatropica.2008.01.003.
39. Klement P, Augustine JM, Delaney KH, Klement G, Weitz JI. 1996. An oral ivermectin regimen that eradicates pinworms (*Syphacia* spp.) in laboratory rats and mice. Lab Anim Sci 46:286–290.
40. Schulz JD, Neodo A, Coulibaly JT, Keiser J. 2018. Development and validation of a LC-MS/MS method for ivermectin quantification in dried blood spots: application to a pharmacokinetic study in *Trichuris trichiura*-infected adults. Anal Methods 10:2901–2909. https://doi.org/10.1039/C8AY00828K.
41. Jaki T, Wolfsegger MJ. 2011. Estimation of pharmacokinetic parameters with the R package PK. Pharm Stat 10:284–288. https://doi.org/10.1002/pst.449.
42. Tucker GT, Houston JB, Huang SM. 2001. Optimizing drug development: strategies to assess drug metabolism/transporter interaction potential—toward a consensus. Clin Pharmacol Ther 70:103–114. https://doi.org/10.1067/mcp.2001.116891.
43. Fenner KS, Troutman MD, Kempshall S, Cook JA, Ware JA, Smith DA, Lee CA. 2009. Drug-drug interactions mediated through P-glycoprotein: clinical relevance and *in vitro-in vivo* correlation using digoxin as a probe drug. Clin Pharmacol Ther 85:173–181. https://doi.org/10.1038/clpt.2008.195.